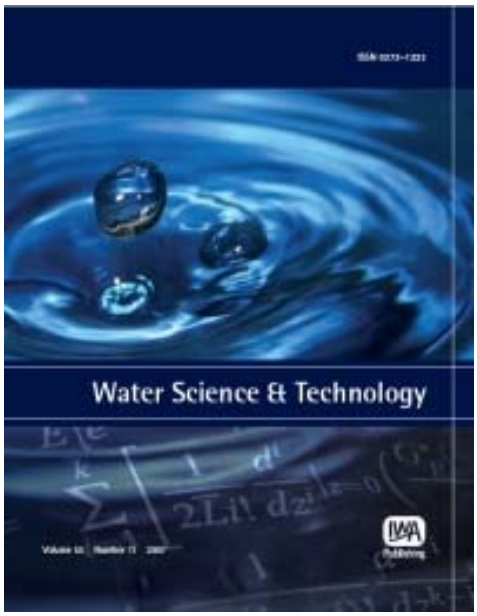

Kinetic modelling of the photocatalytic inactivation of bacteria

Javier Marugán, Rafael van Grieken, Alberto E. Cassano and Orlando M. Alfano

ABSTRACT

This work analyzes the kinetic modelling of the photocatalytic inactivation of *E. coli* in water using different types of kinetic models; from an empirical equation to an intrinsic kinetic model including explicit radiation absorption effects. Simple empirical equations lead to lower fitting errors, but require a total of 12 parameters to reproduce the results of four inactivation curves when the catalyst concentration was increased. Moreover, these parameters have no physical meaning and cannot be extrapolated to different experimental conditions. The use of a pseudo-mechanistic model based on a simplified reaction mechanism reduces the number of required kinetic parameters to 6, being the kinetic constant the only parameter that depends on the catalyst concentration. Finally, a simple modification of a kinetic model based on the intrinsic mechanism of photocatalytic reactions including explicit radiation absorption effects achieved the fitting of all the experiments with only three parameters. The main advantage of this approach is that the kinetic parameters estimated for the model become independent of the irradiation form, as well as the reactor size and its geometrical configuration, providing the necessary information for scaling-up and design of commercial-scale photoreactors for water disinfection.

Key words | disinfection, *Escherichia coli*, kinetics, photocatalysis

Javier Marugán (corresponding author)
Rafael van Grieken
Department of Chemical and Environmental Technology,
ESCET, Universidad Rey Juan Carlos,
C/Tulipán s/n,
28933 Móstoles (Madrid),
Spain
E-mail: *javier.marugan@urjc.es*

Alberto E. Cassano
Orlando M. Alfano
Instituto de Desarrollo Tecnológico para la Industria Química (INTEC),
Universidad Nacional del Litoral-CONICET,
Paraje El Pozo. Ruta Nacional N° 168,
3000 Santa Fe,
Argentina

INTRODUCTION

Application of semiconductor photocatalysis for the oxidation of many organic chemical pollutants in water has been extensively studied in the last decades. More recently, photocatalytic technologies have been also applied to the inactivation of microorganisms with disinfection purposes (Matsunaga *et al.* 1985; Herrera Melián *et al.* 2000; Huang *et al.* 2000; Rincón *et al.* 2001; Dunlop *et al.* 2002; McCullagh *et al.* 2007). These processes have the advantage of avoiding the formation of carcinogenic and mutagenic chloro-organic disinfection byproducts derived from conventional chlorination processes for disinfection of water (Gopal *et al.* 2007).

Several research groups have reported the application of semiconductor photocatalysis to the inactivation of different kinds of pathogenic microorganisms, such as bacteria, viruses, algae, fungi or protozoa (McCullagh *et al.* 2007). Most of the photocatalytic disinfection studies have been mainly focused on the well-known *Escherichia coli* bacterium, whose presence is a widely used indicator of the faecal contamination of water. Some contributions report the effect of operational parameters such as light intensity and titanium dioxide concentration (Horie *et al.* 1996; Benabbou *et al.* 2007), the use of solar light (Fernández *et al.* 2005) and the influence of the chemical composition of water (Rincón & Pulgarín 2004). In most cases, the disinfection concentration profiles show very complex dependences with time, which cannot be successfully described by the simple log-linear Chick's Law. In a previous work (Marugán *et al.* 2008*a*), it has been reported the development of a kinetic model based on a simplified

doi: 10.2166/wst.2010.057

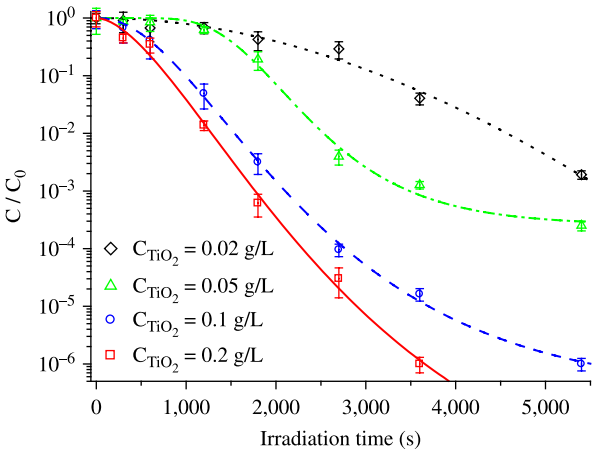

Figure 1 | Experimental results (symbols) and model fitting with Equation (1) (lines) of the photocatalytic inactivation of *E. coli* in water.

inactivation mechanism that was able to fit the disinfection results data over a wide range of experimental conditions using 3 kinetic parameters with well-defined physical meaning. However, this model does not include explicitly the effect of the catalyst concentration and the radiation absorption steps and, consequently, lacks the possibility of generalized applicability.

This work is focused on the kinetic analysis of the photocatalytic inactivation of *E. coli* in water using different types of kinetic models; from an empirical equation to an intrinsic kinetic model with explicit radiation absorption effects. The latter approach has been successfully validated for the photocatalytic oxidation of chemical pollutants such as 4-chlorophenol (Satuf *et al.* 2007) and cyanide (Marugán *et al.* 2008*b*) but to the best of our knowledge there are no references in the literature to the application of this kind of models – an extension of pollutant degradation models – to the inactivation of microorganisms. The main advantage of this approach is that the kinetic parameters estimated for the model are independent of the irradiation form, as well as the reactor size and its geometrical configuration, providing the necessary information for scaling-up and design of commercial-scale photoreactors for water disinfection.

METHODS

Photocatalytic experiments were carried out using commercial Degussa P25 titanium dioxide suspensions. The experimental setup consists of an annular photoreactor of 188.5 cm^3 operating in a closed recirculating circuit driven by a centrifugal pump, with a stirred reservoir tank equipped with a device for withdrawal of samples. The total working volume was 1 L, being the recirculation flow rate of 2.5 L min^{-1}. Illumination was carried out using a Philips TL 6-W black light lamp placed in the axis of the reactor. The lamp provides a nominal UV-A radiation power of 0.7 W with a maximum emission peak centred at 365 nm. More details of the experimental setup can be found elsewhere (van Grieken *et al.* 2009*a*,*b*).

Escherichia coli K12 strains were used to prepare the bacterial suspensions. Fresh liquid cultures were prepared by inoculation in a Luria-Bertani (LB) nutrient medium and incubation at 37°C for 24 h under constant stirring on a rotary shaker. 5 mL of this mother culture were centrifuged for 15 minutes at 3,000 rpm and rinsed with sterile water. This sequence was repeated twice, and finally 1 mL of the microorganisms' suspension was added to water and made up to 1 L to achieve the initial concentration of 10^6 CFU mL^{-1} used in all the experiments. The analysis of the samples along the reaction was carried out following a standard serial dilution procedure in which 0.1 mL of sample are added to 0.9 mL of sterile water and mixed.

Table 1 | Best fitting kinetic parameters for the modified Hom equation (Equation (1))

Exp.	C_{cat} (g L^{-1})	k_1 (-)	k_2 (s^{-1})	k_3 (-)	SSE*
1	0.02	5.41 ± 4.02	(1.86 ± 1.62) × 10^{-2}	3.48 ± 2.19	0.0444
2	0.05	3.59 ± 0.15	(1.22 ± 0.18) × 10^{-3}	12.5 ± 4.88	0.0525
3	0.10	6.54 ± 0.20	(6.02 ± 0.55) × 10^{-4}	2.35 ± 0.22	0.0242
4	0.20	8.74 ± 1.73	(4.59 ± 1.68) × 10^{-4}	1.82 ± 0.38	0.0851
				Total SSE*:	0.2062

*Sum of squared errors computed from the decimal logarithms of the bacterial concentrations.
Note: Errors have been estimated for a 95% confidence interval.

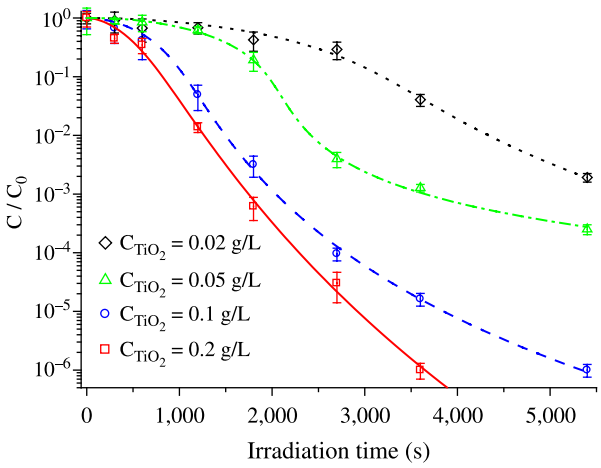

Figure 2 | Experimental results (symbols) and individual series-event model fitting with Equations (3) and (4) (lines) of the photocatalytic inactivation of *E. coli* in water.

This sequence is repeated 3 times to reach bacterial concentrations sufficiently low to be counted. Each decimal dilution was spotted 8 times on LB nutrient agar plates and incubated at 37°C for 24 h before counting.

RESULTS AND DISCUSSION

Kinetic modelling based on empirical equations

Figure 1 shows the results of the photocatalytic inactivation of *E. coli* aqueous suspensions using Degussa P25 TiO_2 with different catalyst loadings.

As it is shown, three different regions can be identified in the plot: i) an initial delay or smooth decay at the beginning of the reaction, usually called "shoulder"; ii) a log-linear inactivation region that covers most part of the reaction; and iii) a deceleration of the process at the end of the process, usually called "tailing". Simple models such as Chick's Law cannot reproduce this complex behaviour. It is required to use equations with at least three parameters to fit the data. Lines in Figure 1 correspond to the fitting to the modified Hom model (Equation (1)).

$$\log\left(\frac{C}{C_0}\right) = -k_1(1 - \exp(-k_2 t))^{k_3} \quad (1)$$

The values of the three kinetic parameters obtained for each experiment are summarized in Table 1. The fitting errors are quite low and the confidence levels for the parameters are reasonable, except for the first experiment in which the end tailing region is not clearly present. However, this model has a clear limitation derived from its empirical nature and the absence of any clear relationship between the parameters and the different variables of the process. Moreover, no clear trends are observed in their values. Consequently, three independent parameters are required for any experiment (twelve in total) and the application of the model is reduced to the experimental range studied being only valid the interpolation on the curve for intermediate experimental times.

Kinetic modelling based on a pseudo-mechanism

The disinfection can be modelled in a simple way by a series events reaction mechanism in which bacteria require a number of incremental damages until become inactivated and finally lysed:

$$C_{\text{undam}} \rightarrow C_{\text{dam}} \rightarrow C_{\text{inact}} \rightarrow C_{\text{prod}} \quad (2)$$

Assuming Langmuir-Hinshelwood-like kinetic models for the reaction rate of every step, the mass balance for

Table 2 | Individual best fitting kinetic parameters for the mechanistic model (Equations (3) and (4))

Exp.	C_{cat} (g L^{-1})	k (CFU mL^{-1} s^{-1})	K (mL^n CFU^{-n})	n (-)	SSE*
1	0.02	$(7.84 \pm 4.84) \times 10^2$	$(4.94 \pm 15.5) \times 10^{-7}$	1.21 ± 0.44	0.0524
2	0.05	$(1.01 \pm 0.07) \times 10^3$	$(4.37 \pm 3.87) \times 10^{-8}$	1.55 ± 0.13	0.0144
3	0.10	$(2.73 \pm 0.88) \times 10^3$	$(6.13 \pm 1.53) \times 10^{-7}$	1.15 ± 0.04	0.0486
4	0.20	$(6.12 \pm 7.68) \times 10^3$	$(5.54 \pm 6.01) \times 10^{-7}$	1.07 ± 0.06	0.0843
				Total SSE*:	0.1997

*Sum of squared errors computed from the decimal logarithms of the bacterial concentrations.
Note: Errors have been estimated for a 95% confidence interval.

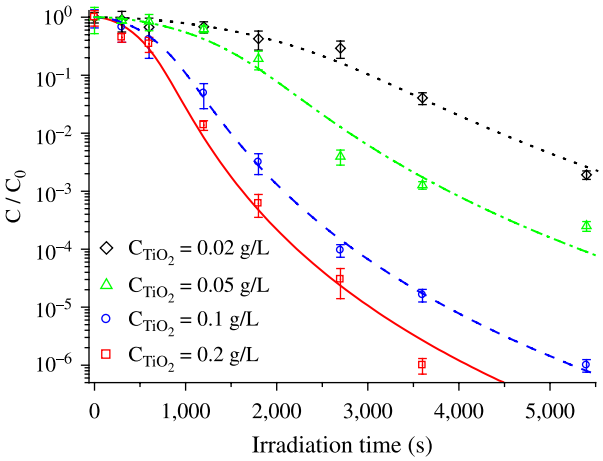

Figure 3 | Experimental results (symbols) and simultaneous series-event model fitting with Equations (3) and (4) (lines) of the photocatalytic inactivation of *E. coli* in water.

both types of viable bacteria can be expressed as follows (Marugán *et al.* 2008*a*):

$$\frac{dC_{undam}}{dt} = -k\frac{KC_{undam}^{n}}{1 + KC_{undam}^{n} + KC_{dam}^{n}} \quad (3)$$

$$\frac{dC_{dam}}{dt} = k\frac{KC_{undam}^{n} - KC_{dam}^{n}}{1 + KC_{undam}^{n} + KC_{dam}^{n}} \quad (4)$$

where k represents a kinetic constant, K a pseudo-adsorption (or interaction) constant, and n is an inhibition coefficient. These three kinetic parameters have a clear physical meaning. They can be obtained by a least-squares fitting of the model to the experimental measurements of the ratio $(C_{undam} + C_{dam})/C_0$ using a non-linear regression algorithm coupled with a numerical integration procedure. Figure 2 shows the fitting curves for each experiment, whereas Table 2 summarizes the values of the kinetic parameters and the fitting errors (even lower than those obtained with the modified-Hom model).

The value of the kinetic constant clearly increases for higher catalyst concentrations, whereas the other two parameters do not show a clear trend. Assuming that only the value of the kinetic constant depends on the catalyst concentration, the values of the pseudo-adsorption constant and the inhibition coefficient can be estimated from the simultaneous fitting of the four experiments, as shown in Figure 3 and Table 3. This approach reduces the number of total parameters from 12 to 6 and narrows their confidence intervals. Although the fitting error of the experiments is higher, the global fitting of all the experiments results more adequate, reducing the obvious overfitting of experiments shown in Figures 1 and 2.

Kinetic modelling based on the intrinsic mechanism

The dependence of the kinetic constant on the catalyst concentration for photocatalytic processes is not directly linear due to the existence of saturation for high catalyst concentrations, where the kinetic constants tend to a maximum asymptotic value that depends on the magnitude of the inlet irradiation flux. For that reason, to consider the effect of the catalyst concentration on the kinetic model, its derivation must be based on an intrinsic photocatalytic reaction mechanism, including the radiation absorption steps and the hydroxyl radicals' generation. The postulated mechanism considers initial reaction steps from the catalyst activation to the hydroxyl radical's generation common to the photocatalytic attack to chemical pollutants. However, the subsequent steps are not elemental but global stages involving several radical attacks. Moreover, due to the large size of bacteria, the interaction TiO_2-bacteria is opposite to the adsorption of chemicals on the TiO_2 surface; i.e. TiO_2 particles are "adsorbed" on the bacteria surface. After some

Table 3 | Simultaneous best fitting kinetic parameters for the mechanistic model (Equations (3) and (4))

Exp.	C_{cat} (g L^{-1})	k (CFU mL^{-1} s^{-1})	K (mL^{n} CFU^{-n})	n (-)	SSE*
1	0.02	$(1.05 \pm 0.32) \times 10^{3}$			0.0826
2	0.05	$(1.65 \pm 0.53) \times 10^{3}$			0.5763
3	0.10	$(3.05 \pm 0.98) \times 10^{3}$	$(6.06 \pm 1.73) \times 10^{-7}$	1.13 ± 0.03	0.0681
4	0.20	$(3.91 \pm 12.4) \times 10^{3}$			0.2652
				Total SSE*:	0.9922

*Sum of squared errors computed from the decimal logarithms of the bacterial concentrations.
Note: Errors have been estimated for a 95% confidence interval.

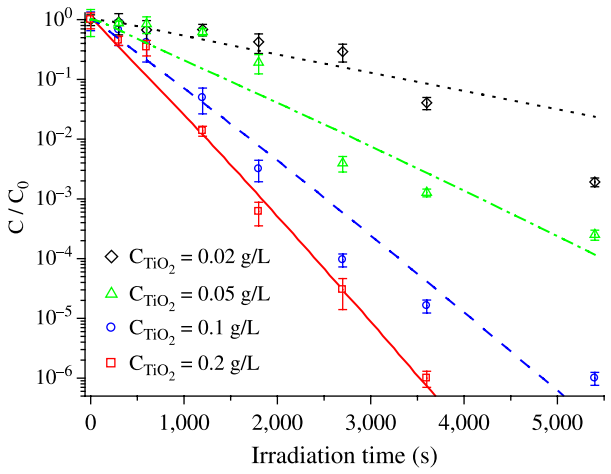

Figure 4 | Experimental results (symbols) and simulation with the intrinsic model of Equations (7) and (8) (lines) of the photocatalytic inactivation of *E. coli* in water.

Table 4 | Best fitting of the parameters for the intrinsic kinetic model (Equations (7) and (8))

Exp.	C_{cat} (g L^{-1})	α'_1 (CFU cm^{-1} s$^{-0.5}$ Einstein$^{-0.5}$)	α_2 (-)	SSE*
1	0.02			1.4141
2	0.05			1.2565
3	0.10	$(4.53 \pm 0.19) \times 10^7$	2.38 ± 0.17	1.5950
4	0.20			0.3383
			Total SSE*:	4.6038

*Sum of squared errors computed from the decimal logarithms of the bacterial concentrations.
Note: Errors have been estimated for a 95% confidence interval.

typical assumptions, the inactivation model represented by Equations (5) and (6) can be derived:

$$\frac{dC_{undam}}{dt} = -\frac{V_R}{V_T} S_g C_{cat} \alpha_1 \times \frac{C_{undam}}{C_{undam} + C_{dam} + \alpha_2 (C_0 - C_{undam} - C_{dam})} \times \left\langle \left[-1 + \sqrt{1 + \frac{\alpha_3 e^a}{S_g C_{cat}}} \right] \right\rangle_{V_R} \quad (5)$$

$$\frac{dC_{dam}}{dt} = \frac{V_R}{V_T} S_g C_{cat} \alpha_1 \times \frac{C_{undam} - C_{dam}}{C_{undam} + C_{dam} + \alpha_2 (C_0 - C_{undam} - C_{dam})} \times \left\langle \left[-1 + \sqrt{1 + \frac{\alpha_3 e^a}{S_g C_{cat}}} \right] \right\rangle_{V_R} \quad (6)$$

where V_R and V_T refer to the reactor and total volume, respectively; C_{cat} is the catalyst concentration, C_0 the initial concentration of bacteria, S_g the catalyst specific surface area, e^a the local volumetric rate of photon absorption and α_1, α_2, and α_3 are lumped kinetic parameters.

A preliminary analysis indicates that under the experimental conditions used in this work $\alpha_3 e^a / S_g C_{cat} \gg 1$. Consequently,

$$\left\langle \left[-1 + \sqrt{1 + \frac{\alpha_3 e^a}{S_g C_{cat}}} \right] \right\rangle_{V_R} \cong \sqrt{\frac{\alpha_3}{S_g C_{cat}}} \left\langle \sqrt{e^a} \right\rangle_{V_R}$$

and, redefining the kinetic parameters as $\alpha'_1 = \alpha_1 \sqrt{\alpha_3}$, the following expressions are obtained:

$$\frac{dC_{undam}}{dt} = -\frac{V_R}{V_T} \sqrt{S_g C_{cat}} \times \alpha'_1 \frac{C_{undam}}{C_{undam} + C_{dam} + \alpha_2 (C_0 - C_{undam} - C_{dam})} \left\langle \sqrt{e^a} \right\rangle_{V_R} \quad (7)$$

$$\frac{dC_{dam}}{dt} = \frac{V_R}{V_T} \sqrt{S_g C_{cat}} \times \alpha'_1 \frac{C_{undam} - C_{dam}}{C_{undam} + C_{dam} + \alpha_2 (C_0 - C_{undam} - C_{dam})} \left\langle \sqrt{e^a} \right\rangle_{V_R} \quad (8)$$

Figure 4 and Table 4 show the plots and values of the kinetic parameters resulting from the fitting of the experimental data with the model.

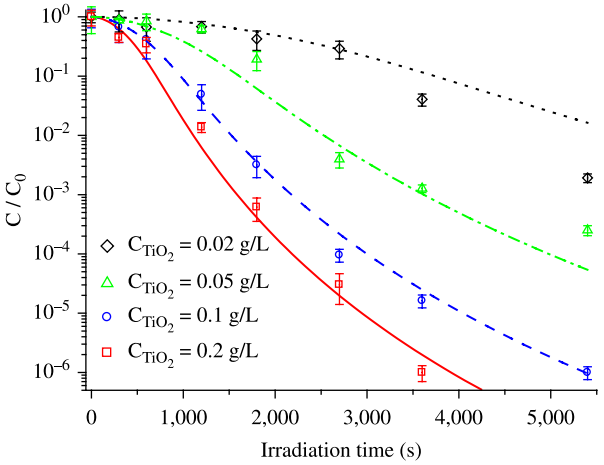

Figure 5 | Experimental results (symbols) and simulation with the intrinsic model of Equations (9) and (10) (lines) of the photocatalytic inactivation of *E. coli* in water.

Table 5 | Best fitting kinetic parameters for the modified intrinsic kinetic model (Equations (9) and (10))

Exp.	C_{cat} (g L^{-1})	α'_1 (CFU cm^{-1} $s^{-0.5}$ $Einstein^{-0.5}$)	α_2 (-)	m (-)	SSE*
1	0.02				1.1093
2	0.05				0.8992
3	0.10	$(1.75 \pm 0.63) \times 10^{7}$	$(3.62 \pm 3.10) \times 10^{-1}$	1.11 ± 0.06	0.1802
4	0.20				0.3754
				Total SSE*:	2.5639

*Sum of squared errors computed from the decimal logarithms of the bacterial concentrations.
Note: Errors have been estimated for a 95% confidence interval.

The number of model parameters is only two and their confidence level is very narrow. In contrast, the global fitting error is now much higher. The reason can be observed in Figure 4. In fact, the model is not able to reproduce the tailing region of the curves, leading to poor fitting of experiments 2 and 3.

That means that the proposed intrinsic reaction mechanism cannot reproduce satisfactorily the shape of the inactivation curves. The cause seems to be the first-order dependence of the reaction rate with the concentration of bacteria. For that reason, a very simple semi-empirical modification of this model, introducing an exponent in the concentration dependences (similar to the inhibition coefficient of Equations (3) and (4), is proposed:

$$\frac{dC_{undam}}{dt} = -\frac{V_R}{V_T}\sqrt{S_g C_{cat}} \times \alpha'_1 \frac{C_{undam}^m}{C_{undam}^m + C_{dam}^m + \alpha_2(C_0^m - C_{undam}^m - C_{dam}^m)} \left\langle \sqrt{e^a} \right\rangle_{V_R} \quad (9)$$

$$\frac{dC_{dam}}{dt} = \frac{V_R}{V_T}\sqrt{S_g C_{cat}} \times \alpha'_1 \frac{C_{undam}^m - C_{dam}^m}{C_{undam}^m + C_{dam}^m + \alpha_2(C_0^m - C_{undam}^m - C_{dam}^m)} \left\langle \sqrt{e^a} \right\rangle_{V_R} \quad (10)$$

Figure 5 shows the curves obtained upon fitting of the experimental data with Equations (9) and (10) (see Table 5 for the values of the kinetic parameters). As it can be seen, this model can successfully describe the three regions of the inactivation curves employing only three parameters with a quite low confidence interval. In this case, the model is able to reasonably fit a total of 31 experimental points. The global fitting error is slightly higher than that of the pseudo-mechanistic model, but it must be noticed that the number of parameters has been reduced from 6 to 3 (and independent of the number of experiments). In addition, what is more important, the dependence of the reaction rate on the catalyst concentration and on the radiation absorption rate has been successfully included in the model.

As it can be seen, the value of the inhibition coefficient m is quite similar to that of the inhibition coefficient n defined in the pseudo-mechanistic model represented by Equations (3) and (4). The physical meaning of this parameter is related to the established competition for the hydroxyl radicals between the organic species released to the medium upon the lysis of the bacterial cells and the surviving microorganisms. Our current efforts are focused on the elucidation of the mechanistic steps from which this inhibition coefficient can be derived.

CONCLUSIONS

The photocatalytic inactivation of *E. coli* suspensions has been successfully modelled with different kinetic equations. Simple empirical equations leads to the lower fitting error, but required a large number of parameters with no physical meaning, and consequently the equations are useless for the extrapolation of the results to other experimental conditions. The use of a pseudo-mechanistic model based on a simplified reaction mechanism leads to a reduction of the number of the required kinetic parameters. The use of parameters with more physical meaning makes that in this case, only the kinetic constant depends on two operational parameters such as the catalyst concentration and the irradiation rate. Finally, a kinetic model based on the intrinsic mechanism of photocatalytic reactions, including the radiation absorption steps and the generation of

hydroxyl radicals, allowed the simulation of the experimental data with only two parameters, including the influence of the catalyst concentration. However, the derived model does not reproduce the tailing region of the inactivation curves, but a simple, semi-empirical modification of the equations by including an inhibition coefficient as the exponent of the bacterial concentrations leads to a very reasonable simultaneous fitting of all the experimental data with only three parameters. The main advantage of this model is that all the parameters have a clear physical meaning. Additionally, it takes into account explicitly the volumetric rate of photon absorption and the catalyst loading, which allows the simulation, design and scaling-up of photocatalytic disinfection reactors with different geometries.

ACKNOWLEDGEMENTS

The authors gratefully acknowledge the financial support of the Ministerio de Educación y Ciencia of Spain through the program Consolider-Ingenio 2010 (project CSD2006-00044 TRAGUA) and Comunidad de Madrid through the program REMTAVARES S-0505/AMB/0395 and from the Universidad Nacional del Litoral, Agencia Nacional de Promoción Científica y Tecnológica, and Consejo Nacional de Investigaciones Científicas y Técnicas of Argentina.

REFERENCES

Benabbou, A. K., Derriche, Z., Felix, C., Lejeune, P. & Guillard, C. 2007 Photocatalytic inactivation of *Escherichia coli*: effect of concentration of TiO_2 and microorganism, nature, and intensity of UV irradiation. *Appl. Catal. B: Environ.* **76**, 257–263.

Dunlop, P. S. M., Byrne, J. A., Manga, N. & Eggins, B. R. 2002 The photocatalytic removal of bacterial pollutants from drinking water. *J. Photochem. Photobiol. A: Chem.* **148**, 355–363.

Fernández, P., Blanco, J., Sichel, C. & Malato, S. 2005 Water disinfection by solar photocatalysis using compound parabolic collectors. *Catal. Today* **101**, 345–352.

Gopal, K., Tripathy, S. S., Bersillon, J. L. & Dubey, S. P. 2007 Chlorination byproducts, their toxicodynamics and removal from drinking water. *J. Hazard. Mater.* **140**, 1–6.

Herrera Melián, J. A., Doña Rodríguez, J. M., Viera Suárez, A., Tello Rendón, E., Valdés do Campo, C., Araña, J. & Pérez Peña, J. 2000 The photocatalytic disinfection of urban waste waters. *Chemosphere* **41**, 323–327.

Horie, Y., David, D. A., Taya, M. & Tone, S. 1996 Effects of light intensity and titanium dioxide concentration on photocatalytic sterilization rates of microbial cells. *Ind. Eng. Chem. Res.* **35**, 3920–3926.

Huang, Z., Maness, P.-C., Blake, D. M., Wolfrum, E. J., Smolinski, S. L. & Jacobi, W. A. 2000 Bactericidal mode of titanium dioxide photocatalysis. *J. Photochem. Photobiol. A: Chem.* **130**, 163–170.

Marugán, J., van Grieken, R., Sordo, C. & Cruz, C. 2008*a* Kinetics of photocatalytic disinfection of *Escherichia coli* suspensions with titania and titania/silica materials. *Appl. Catal. B: Environ.* **82**, 27–36. Corrigendum: *Appl. Catal. B: Environ.* **88**, 582–583.

Marugán, J., van Grieken, R., Cassano, A. E. & Alfano, O. M. 2008*b* Intrinsic kinetic modeling with explicit radiation absorption effects of the photocatalytic oxidation of cyanide with TiO_2 and silica-supported TiO_2 suspensions. *Appl. Catal. B: Environ.* **85**, 48–60.

Matsunaga, T., Tomoda, R., Nakajima, T. & Wake, H. 1985 Photoelectrochemical sterilization of microbial cells by semiconductor powders. *Fems Microbiol. Lett.* **29**, 211–214.

McCullagh, C., Robertson, J. M. C., Bahnemann, D. W. C. & Robertson, P. K. J. 2007 The application of TiO_2 photocatalysis for disinfection of water contaminated with pathogenic micro-organisms: a review. *Res. Chem. Intermediat.* **33**(3–5), 359–375.

Rincón, A. G. & Pulgarín, C. 2004 Effect of pH, inorganic ions, organic matter and H_2O_2 on *E. coli* K12 photocatalytic inactivation by TiO_2: Implications in solar water disinfection. *Appl. Catal. B: Environ.* **51**, 283–302.

Rincón, A. G., Pulgarín, C., Adler, N. & Peringer, P. 2001 Interaction between *E. coli* inactivation and DBP-precursors - dihydroxybenzene isomers- in the photocatalytic process of drinking-water disinfection with TiO_2. *J. Photochem. Photobiol. A: Chem.* **139**, 233–241.

Satuf, M. L., Brandi, R. J., Cassano, A. E. & Alfano, O. M. 2007 Scaling-up of slurry reactors for the photocatalytic degradation of 4-chlorophenol. *Catal. Today* **129**, 110–117.

van Grieken, R., Marugán, J., Sordo, C. & Pablos, C. 2009*a* Comparison of the photocatalytic disinfection of *E. coli* suspensions in slurry, wall and fixed-bed reactors. *Catal. Today* **144**, 48–54.

van Grieken, R., Marugán, J., Sordo, C., Martínez, P. & Pablos, C. 2009*b* Photocatalytic inactivation of bacteria in water using suspended and immobilized silver-TiO_2. *Appl. Catal. B: Environ.* **93**, 112–118.